Testing quantum mechanics within the realm of quantum mechanics

Matthieu ARACTINGI, Jacques ROBERT

Université Paris-Saclay, CNRS,
Laboratoire de physique des gaz et des plasmas, 91405, Orsay, France
email: jacques.robert@universite-paris-saclay.fr

ABSTRACT. It is shown that the two models of quantum mechanics, the spectral model (SM) and the fluid model (FM), do not necessarily lead to the same expression for the velocity distribution of a coherent matter-wave beam, such as atoms. Consequently, we propose at least one type of experiment that yields different results depending on the model used.

RÉSUMÉ. On montre que les deux modèles de la mécanique quantique, le modèle spectral (MS) et le modèle fluide (MF) , ne conduisent pas nécessairement à la même expression pour la distribution des vitesses d'un faisceau cohérent d'ondes de matière, tel que des atomes. En conséquence, on propose au moins un type d'expérience qui aboutit à des résultats différents selon le modèle utilisé.

P.A.C.S.: 03.65.–w; 03.75-b

1 Introduction

Quantum mechanics can be described in various ways, but generally, it follows two models (which we will call for simplicity): the Spectral Model (SM) (Heisenberg, Schrödinger, Darwin, Kennard, etc.) and the Fluid Model (FM) or hydrodynamical (de Broglie, Madelung, Bohm, etc.). One of the points of deBroglie-Bohm mechanics, is to incorporate particle trajectories into the standard quantum framework. While this interpretation gives a concrete meaning to fluid trajectories, its predictions are still constrained by the probabilistic nature of initial conditions, leaving it no more predictive than conventional quantum theory. In certain instances, the fluid trajectory may even differ from the reconstructed path. Thus far, the debate between these two models has mainly focused on solutions regarding the measurement of particle positions to reconstruct "trajectories" and their relationship to classical trajectories as in experiments with light [30]. But this article addresses another perspective.

This article is motivated by the discomfort related to breaking the inertia principle [1], in this quote one has to remind that L. de Broglie considered photons as particles. This discomfort leads to the "surreal" nature of fluid solutions [2, 3] when compared to particle-based solutions [4, 5, 6, 7]. In this article, we show that these two models do not always agree on velocity distribution predictions, for non relativistic massive particles. Specifically, in the context of diffraction, we demonstrate that near the slits, the two models significantly differ but converge to the same velocity distribution at a distance. This raises questions about the physical meaning of velocity in both models. In the next section, we propose a series of laser spectroscopy experiments, sensitive to the

[1] [1]p. 549, l. 6 "Les atomes de lumière dont nous admettons l'existence ne se propagent pas toujours en ligne droite, comme le prouvent les phénomènes de diffraction. Il semble donc nécessaire de modifier le principe de l'inertie. Nous proposons de mettre à la base de la dynamique du point matériel libre le postulat suivant: 'En chaque point de sa trajectoire, un mobile libre suit d'un mouvement uniforme le rayon de son onde de phase, c'est-à-dire (dans un milieu isotrope) la normale aux surfaces d'égale phase'. En général, le mobile suivra donc la trajectoire rectiligne fixée par le principe de Fermat appliqué à l'onde de phase, qui se confond ici avec le principe de moindre action appliqué au mobile sous la forme Maupertuisienne. Mais si le mobile doit traverser une ouverture dont les dimensions sont petites par rapport à la longueur d'onde de l'onde déphasée, sa trajectoire se courbera général comme le rayon de l'onde diffractée. La conservation de l'énergie est sauve, mais non celle de la quantité de mouvement, à moins qu'il ne se transmette une pression aux atomes matériels formant le bord de l'ouverture."

Doppler effect on a spatially coherent atomic beam with a Gaussian profile, to differentiate between these models. This will allow testing quantum mechanics through a strictly quantum measurement.

2 Spectral Model and Fluid Model of Quantum Mechanics

We consider the simplest case of the free movement of a particle of mass m in space. We can consider two possible representations of the wave function $\psi(\overrightarrow{x},t)$, that are solutions of the Schrödinger equation:

$$i\frac{h}{2\pi}\frac{\partial\psi(\overrightarrow{x},t)}{\partial t} = H(\overrightarrow{x},\overrightarrow{p},t)\psi(\overrightarrow{x},t) \tag{1}$$

By construction , the wave function is considered to represent a wave field [8, 9].

The Spectral Model corresponds to the development of the wave function as a sum of modes with a set of functions $a_i(\overrightarrow{x})$ (usually orthonormal for the Hilbert product) and $s_i(\overrightarrow{x},t)$, which can be taken as real [10, 11, 12]:

$$\psi(\overrightarrow{x},t) = \sum_i a_i(\overrightarrow{x})e^{i\frac{2\pi}{h}s_i(\overrightarrow{x},t)} \tag{2}$$

The sum over the indices "i" can be discrete or continuous.

The Fluid Model however[13, 14] , corresponds to the parameterization of the wave function by Louis de Broglie in the "amplitude-phase" form. With two real functions $R(\overrightarrow{x},t)$ being the amplitude and $S(\overrightarrow{x},t)$ the phase:

$$\psi(\overrightarrow{x},t) = R(\overrightarrow{x},t)e^{i\frac{2\pi}{h}S(\overrightarrow{x},t)} \tag{3}$$

3 Probability Density Fields, Flux Density , and Velocity Fields

In both expressions, the complex nature of the wave function is present but expressed differently through two quantities $\rho(\overrightarrow{x},t)$ and $\overrightarrow{j}(\overrightarrow{x},t)$. Where

$$\rho(\overrightarrow{x},t) = \left|\psi(\overrightarrow{x},t)\right|^2 \tag{4}$$

is the probability density, and

$$\overrightarrow{j}(x,t) = i\frac{h}{4\pi m}\left\{\psi(\overrightarrow{x},t)\overrightarrow{\nabla}_{\overrightarrow{x}}\psi^*(\overrightarrow{x},t) - \psi^*(\overrightarrow{x},t)\overrightarrow{\nabla}_{\overrightarrow{x}}\psi(\overrightarrow{x},t)\right\} \tag{5}$$

is the probability flux density . These quantities, are derived by rewriting Schrödinger's equation associated with the conservation equation of the probability density of particle presence:

$$\frac{\partial \rho(\overrightarrow{x},t)}{\partial t} + \overrightarrow{\nabla}_{\overrightarrow{x}}.\overrightarrow{j}(\overrightarrow{x},t) = 0 \tag{6}$$

According to Madelung [14], and as reiterated by Landau [15], writing

$$\overrightarrow{j}(\overrightarrow{x},t) = \rho(\overrightarrow{x},t)\overrightarrow{v}(\overrightarrow{x},t) \tag{7}$$

defines the velocity field in the Fluid Model. We note that the velocity field can be computed very simply with the FM as [16, 17]:

$$\overrightarrow{v}(\overrightarrow{x},t) = \frac{1}{m}\overrightarrow{\nabla}_{\overrightarrow{x}}S(\overrightarrow{x},t) = \frac{h}{2\pi m}Im\left(\frac{\overrightarrow{\nabla}_{\overrightarrow{x}}\psi(x,t)}{\psi(x,t)}\right) \tag{8}$$

The velocity field is thus naturally related to the complex nature of the wave function. One could note that a set of trajectories can directly be associated to the Fluid Model based on the velocity field [1, 17, 20] .

The expression for the probability density is written in both models as:

$$\rho(\overrightarrow{x},t) = |\psi(\overrightarrow{x},t)|^2 = \begin{cases} \left|\sum_i a_i(\overrightarrow{x})e^{i\frac{2\pi}{h}s_i(\overrightarrow{x},t)}\right|^2 \\ R^2(\overrightarrow{x},t) \end{cases} \tag{9}$$

Since both models lead to the same result, it is not possible through measurements of $\rho(\overrightarrow{x},t)$, i.e., the number of particles arriving near a defined position, to determine which model is more relevant. The Heisenberg uncertainty relations govern in this case the link between the uncertainty in the measured position distribution and the associated velocity distribution.

For the velocity distribution, the Spectral Model [11] derives the momentum distribution $\varrho(\overrightarrow{p},t)$ from the Fourier transform of the wave function:

$$\varrho(\overrightarrow{p},t) = |\phi(\overrightarrow{p},t)|^2 = \left|\int_{-\infty}^{+\infty} e^{-i2\pi\frac{\overrightarrow{p}.\overrightarrow{x}}{h}}\psi(\overrightarrow{x},t)\,d^3\overrightarrow{x}\right|^2 \tag{10}$$

This result is widely used, for example, in expressing line shapes in a gas, such as the Voigt profile, which describes the line shape obtained

by sweeping the frequency ω associated with the laser wave vector $\overrightarrow{k}$ around a narrow resonance ω_0, with width γ and shift δ [18]:

$$I(\omega) = \int d\overrightarrow{v}\ \rho(\overrightarrow{v}) \frac{\gamma/\pi}{\gamma^2 + (\omega - \omega_0 - \delta - \overrightarrow{k}.\overrightarrow{v})^2} \tag{11}$$

where $\rho(\overrightarrow{v}) = m\rho(\overrightarrow{p}/m)$.

This expression can be refined by including recoil effects and the laser beam profile [19].

To our knowledge, the expression for the velocity distribution corresponding to the fluid model does not appear to have been established or used. We will provide it in the simple and analytical case of a Gaussian slit acting in a direction transversal to the main longitudinal motion as in [4], This slit model can be considered as a realistic one as it contains evanescent waves contributions [25, 26]

To evaluate the "real" nature of quantum trajectories, a useful first step is to test whether the corresponding velocity distribution produces observable effects, such as a specific Doppler profile. These profiles are common experimental measurements in atomic or molecular beams since the availability of high resolution scannable quasi-resonnant laser sources, some illustrations can be found in [27, 28, 29]. In the present case the atomic beam is taken as a solution of the Schrödinger's equation, corresponds to a pure case ans as such exhibits coherence properties.

However, it seems that the inclusion of the expression for $\rho(\overrightarrow{v})$ corresponding to the fluid model in equation (11) is absent from the literature. More crucially, there has been no analysis of the potential consequences of any difference between the two models when comparing their velocity distributions. This is the point that we wish to develop further in this article.

We will revisit the Voigt formula in the specific, yet generic, case of Gaussian atomic waves [4]. To do this, we will first recall the form of the velocity distribution in the Spectral Model and then establish the one obtained in the Fluid Model. It is important to note that in both cases, we remain consistent with Heisenberg's uncertainty principle, as we are not attempting to simultaneously measure the associated position distribution.

4 Velocity Distributions and Spectral Model or Fluid Model for a One-Dimensional Gaussian Wave

4.1 Form of the Velocity Distribution in Both Models

Let us firstly consider the calculation in the case of the spectral model.

Let $H = \frac{p^2}{2m}$ the Hamiltonian associated with one-dimensional free motion, forms the solution

$$\psi(x,t) = \int_{-\infty}^{+\infty} e^{i2\pi \frac{px - \frac{p^2}{2m}t}{h}} \phi(p)\, dp \tag{12}$$

Following Heisenberg [10, 11, 12], we take as the initial function $f(x)$ a wave packet of the form of a "plane wave passing through x_0 at $t = 0$" modulated by a (unnormalized) Gaussian distribution centered at x_0:

$$f(x) = \exp\left[-\frac{1}{2\sigma^2}(x - x_0)^2 + i\frac{2\pi}{h}mv(x - x_0)\right] \tag{13}$$

This is the widely used model of the Gaussian slit. The corresponding initial intensity is thus distributed following

$$\rho(x,0) = \exp\left[-\frac{1}{\sigma^2}(x - x_0)^2\right] \tag{14}$$

To determine $\phi(p)$, we evaluate (12) at $t = 0$:

$$f(x) = \psi(x,0) = \int_{-\infty}^{+\infty} e^{i2\pi \frac{px}{h}} \phi(p)\, dp = e^{-\frac{1}{2\sigma^2}(x - x_0)^2 + i\frac{2\pi}{h}mv(x - x_0)} \tag{15}$$

After the usual manipulations, the wave function in the "p" representation is therefore:

$$\varphi(p,t) = \frac{\sigma\sqrt{2\pi}}{\sqrt{h}} e^{\left[-\frac{1}{\left(\frac{h}{2\pi\sigma}\right)^2}(p - mv)^2 - i\frac{2\pi}{h}p\left(x_0 + \frac{p}{2m}t\right)\right]} \tag{16}$$

and the probability density in the "p" representation is

$$\varrho(p,t) = \frac{\sigma^2 2\pi}{h} e^{\left[-\frac{1}{\left(\frac{h}{2\pi\sigma}\right)^2}(p - mv)^2\right]} \tag{17}$$

The "p" representation is the representation of the spectral model, and $m\varrho(p/m,t) = \varrho_s(v_s)$, where $v_s = p/m$ is the corresponding velocity distribution. In this expression, the variable t has disappeared.

We can substitute the expression for $\phi(p)$ into (12) and, after calculation, we get

$$\psi(x,t) = \frac{\sigma}{\sqrt{\left(\sigma^2 + i\frac{ht}{2\pi m}\right)}} e^{\left[-\frac{1}{2}\frac{(x-x_0-vt)^2}{\left(\sigma^2+i\frac{ht}{2\pi m}\right)} + i\frac{2\pi}{h}mv\left(x-x_0-\frac{v}{2}t\right)\right]} \tag{18}$$

One can verify through direct calculation that this expression satisfies the wave equation with an energy represented by a complex number that reflects the dispersion in momentum mv.

Finally, The probability density is

$$\rho(x,t) = \frac{\sigma}{\sqrt{\sigma^2 + \left(\frac{ht}{2\pi m\sigma}\right)^2}} \exp\left[-\frac{(x-x_0-vt)^2}{\sigma^2 + \left(\frac{ht}{2\pi m\sigma}\right)^2}\right] \tag{19}$$

It is relevant to note that the exponential term in $\psi(x,t)$ highlights the contribution of the "wave packet spreading term" in the "x" representation:

$$-\frac{1}{2}\frac{(x-x_0-vt)^2}{\left(\sigma^2 + i\frac{ht}{2\pi m}\right)} + i\frac{2\pi}{h}mv\left(x-x_0-\frac{v}{2}t\right) \tag{20}$$

We can separate the real and imaginary parts as:

$$-\frac{1}{2}\frac{(x-x_0-vt)^2}{\sigma^2 + \left(\frac{ht}{2\pi m\sigma}\right)^2} + i\left(\frac{1}{2}\frac{(x-x_0-vt)^2}{\sigma^2 + \left(\frac{ht}{2\pi m\sigma}\right)^2}\frac{ht}{2\pi m\sigma^2} + \frac{2\pi}{h}mv\left(x-x_0-\frac{v}{2}t\right)\right) \tag{21}$$

Let us now consider the fluid model. With the "phase-amplitude" parameterization (3):

$$\psi(x,t) = R(x,t)e^{i\frac{2\pi}{h}S(x,t)}$$

we note $\sqrt{\left(\sigma^2 - i\frac{ht}{2\pi m}\right)} = r(t)e^{-i\theta(t)}$ where $\tan(2\theta(t)) = \frac{ht}{2\pi m\sigma^2}$:

$$R(x,t) = \frac{\sqrt{\sigma}}{\sqrt[4]{\left(\sigma^2 + \left(\frac{ht}{2\pi m\sigma}\right)^2\right)}} \exp\left[-\frac{1}{2}\frac{(x-x_0-vt)^2}{\sigma^2 + \left(\frac{ht}{2\pi m\sigma}\right)^2}\right] \tag{22}$$

$$S(x,t) = \frac{h}{2\pi}\theta(t) + mv\left(x - x_0 - \frac{v}{2}t\right) + \frac{mt}{2}\frac{(x - x_0 - vt)^2}{\sigma^2 + \left(\frac{h}{2\pi m\sigma}\right)^2 t^2}\left(\frac{h}{2\pi m\sigma}\right)^2 \tag{23}$$

We can then determine the velocity, or rather the **velocity field of the fluid model**, or hydrodynamic model [14], with (8) for one dimension as:

$$v_f(x,t) = \frac{1}{m}\partial_x S(x,t) = v + t\frac{(x - x_0 - vt)}{\sigma^2 + \left(\frac{h}{2\pi m\sigma}\right)^2 t^2}\left(\frac{h}{2\pi m\sigma}\right)^2 \tag{24}$$

To determine the equivalent velocity distribution with (19), one must invert (24) and satisfy

$$\rho(v_f,t)dv_f = \rho(v_f,t)dv_f(x,t) = \rho(x,t)dx \tag{25}$$

The variable change is obtained with

$$(x - x_0 - vt) = \frac{\left(\sigma^2 + \left(\frac{ht}{2\pi m\sigma}\right)^2\right)t}{\left(\frac{ht}{2\pi m\sigma}\right)^2}(v_f - v) \tag{26}$$

The Jacobian $J(t)$ with $dv_f(x,t) = J(t)dx$ is:

$$J(t) = \frac{\partial v_f(x,t)}{\partial x} = \frac{\left(\frac{h}{2\pi m\sigma}\right)^2 t}{\sigma^2 + \left(\frac{h}{2\pi m\sigma}\right)^2 t^2}$$

Finally,

$$\rho_f(v_f,t) = \frac{t\sigma\sqrt{\sigma^2 + \left(\frac{ht}{2\pi m\sigma}\right)^2}}{\left(\frac{ht}{2\pi m\sigma}\right)^2}\exp\left[-\frac{\left(\sigma^2 + \left(\frac{ht}{2\pi m\sigma}\right)^2\right)t^2}{\left(\frac{ht}{2\pi m\sigma}\right)^4}(v_f - v)^2\right] \tag{27}$$

This result, which motivates this study, should be compared with the previously obtained probability density given by eq:(17):

$$\varrho_s(v_s) = \frac{m\sigma^2 2\pi}{h}e^{\left[-\frac{m^2}{\left(\frac{h}{2\pi\sigma}\right)^2}(v_s - v)^2\right]}$$

we can clearly see the difference between the two models as we will detail in the following section.

4.2 Study of Limits as a Function of t

Since the spectral model has a velocity distribution that is independent of time, we want to consider the limit cases in order to compare their distributions.

Lets us first consider the case when $t \gg \frac{2\pi m\sigma^2}{h}$:

$$\rho_f(v_f,t) \underset{t\gg\frac{2\pi m\sigma^2}{h}}{=} \frac{2\pi m\sigma^2}{h} \exp\left[-\frac{m}{\left(\frac{h}{2\pi\sigma}\right)^2}(v_f-v)^2\right] \tag{28}$$

In this limit, we find that both models are coherent with one another, i.e $\rho_s(v_s) = \rho_f(v_f, t \to \infty)$. **We will define the limit where $t \gg \frac{2\pi m\sigma^2}{h}$ as a far-field limit. And therefore correspond to the limit where the two distributions coincide.**

Lets us now consider the case when $t \ll \frac{2\pi m\sigma^2}{h}$:

$$\rho_f(v_f,t) \underset{t\ll\frac{2\pi m\sigma^2}{h}}{=} \left(\frac{2\pi m\sigma^2}{h}\right)^2 \frac{1}{t} \exp\left[-\frac{1}{2}\frac{(v_f-v)^2}{\left(\frac{h}{2\pi m\sigma^2}\right)^4 \frac{\sigma^2t^2}{2}}\right]$$

$$\rho_f(v_f,t) \underset{t\ll\frac{2\pi m\sigma^2}{h}}{=} \frac{\sqrt{2\pi}\sigma}{\sqrt{2}}\left[\left(\frac{2\pi m\sigma^2}{h}\right)^2 \frac{1}{t}\frac{\sqrt{2}}{\sqrt{2\pi}\sigma} \exp\left[-\frac{1}{2}\frac{(v_f-v)^2}{\left(\frac{h}{2\pi m\sigma^2}\right)^4 \frac{\sigma^2t^2}{2}}\right]\right] \tag{29}$$

where the term inside [ ] is of the form

$$f(x) = \frac{1}{\sqrt{2\pi}\beta} e^{-\frac{1}{2}\frac{(x-x_0)^2}{\beta^2}} \underset{\beta\to 0}{\longrightarrow} \delta(x-x_0) \tag{30}$$

Consequently, the probability density function $\rho_f(v_f, t)$ evolves into a delta function as well:

$$\rho_f(v_f,t) \underset{t\ll\frac{2\pi m\sigma^2}{h}, t\to 0}{=} \sqrt{\pi}\sigma\ \delta(v_f-v) \tag{31}$$

and if $v = 0$, we have

$$\rho_f(v_f,t) \underset{t\ll\frac{2\pi m\sigma^2}{h}, t\to 0}{=} \sqrt{\pi}\sigma\ \delta(v_f) \tag{32}$$

while the spectral model always leads to:

$$\varrho_s(v_s) = \frac{m\sigma^2 2\pi}{h} e^{\left[-\frac{m^2}{\left(\frac{h}{2\pi\sigma}\right)^2}(v_s - v)^2\right]}$$

We see that in this limit, the two velocity distributions do not match, demonstrating a fundamental difference between the spectral and fluid models in the near field limit. This result is illustrated in the following figure :

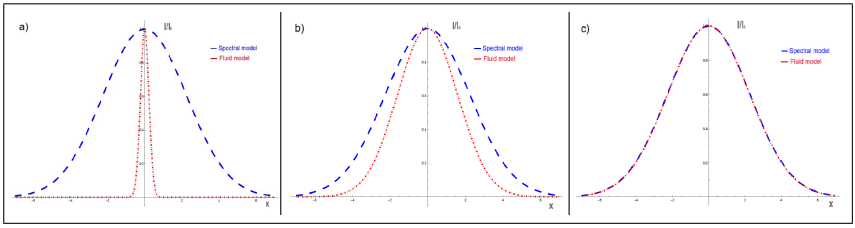

Figure 1: Plot of the velocity distribution of the two models after passing through a slit for near-field (a), intermediate (b), and far-field (c) regimes.

As we can see , there is a converges of the two model from the near field to the far field regime.

The difference between these distributions in the near field regime is the main result that this article aimed to illustrate.

5 Experimental Test Using Line Shapes

With the two models previously established, it is possible to conduct experiments using laser beams in near-field, intermediate, or far-field positions, as indicated in a pictural way in Figure 2.

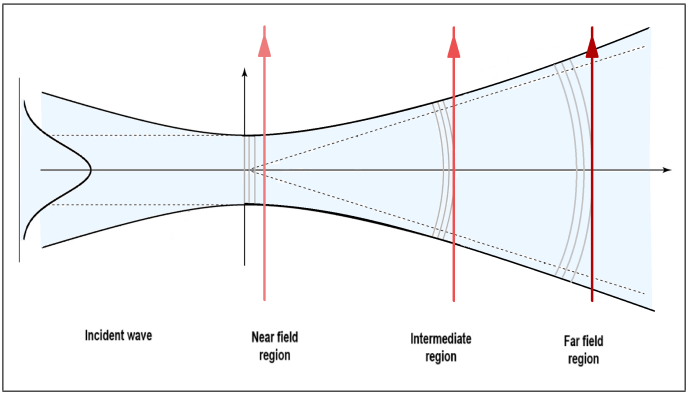

Figure 2: Pictural representation of the principle of a laser spectroscopy experiment on a Gaussian atomic jet to test the velocity distribution at different positions relative to the jet's nozzle.

We can see in Figure 2 that, if the laser beam propagates along the x-axis, $\overrightarrow{k} = k\overrightarrow{u}_x$, perpendicular to the atomic beam propagating along the z-axis (where $z = v_z t$), we can probe the width of the velocity distribution along x and of the atomic beam at various positions in z , by laterally moving the laser beam. One can choose any other configuration that allows probing of the velocity distribution $\rho_z(v_x)$ in near-field or far-field regimes.

Representing the atomic beam with a transverse Gaussian profile, with width σ_x at $z = 0$, assumes that this atomic beam is spatially coherent in the x direction. The line profile $I_x(\omega)$ is expressed by:

$$I_x(\omega, z) = \int dv_x \, \rho_z(v_x) \frac{\gamma/\pi}{\gamma^2 + (\omega - \omega_0 - \delta - kv_x)^2}$$

If we adopt the spectral model:

$$\rho_z(v_x) = \frac{\sigma_x^2 2\pi}{h} e^{\left[-\frac{1}{\left(\frac{h}{2\pi\sigma_x}\right)^2}(p_x/m)^2\right]}$$

then $I_x(\omega, z) \equiv I_x^s(\omega)$ is independent of z, and if the Lorentzian line width is sufficiently narrow, the signal will be primarily Gaussian and will reproduce the momentum distribution regardless of the position of the laser.

If we adopt the fluid model, with $t = z/v_z$, for a monokinetic atomic beam along v_z:

$$\rho(v_{fx}(z), z) \underset{z \ll \frac{2\pi m \sigma^2}{h} v_z, z \to 0}{=} \frac{\sqrt{2\pi}\sigma}{\sqrt{2}} \delta\left(v_{fx}\right)$$

$$I_x^F(\omega) = \frac{\sqrt{2\pi}\sigma}{\sqrt{2}} \frac{\gamma/\pi}{\gamma^2 + (\omega - \omega_0 - \delta)^2}$$

The Voigt profile for the fluid model in the near-field reduces to the Lorentzian profile, while the Voigt profile in the far-field matches that of the spectral model, which is the same regardless of the value of z.

Thus, one can differentiate experimentally between the two main models used in quantum mechanics, the spectral model and the fluid model, by conducting a series of laser spectroscopy experiments sensitive to the Doppler effect on a spatially coherent Gaussian profile atomic beam.

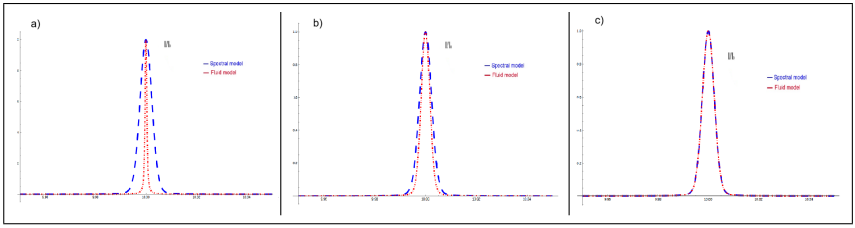

Figure 3: Plot of the Voigt profile (for $\gamma = \sigma/100$) of the two models after passing through a slit for near-field (a), intermediate (b), and far-field (c) regimes.

6 Double Gaussian Slit

The previous method can be applied to the case of two Gaussian slits, one centered at $+x_0$ and the other at $-x_0$. The amplitude is evenly distributed between the two slits. To determine $\phi(p)$, we write Equation (15) at $t = 0$:

$$f(x) = \frac{1}{\sqrt{2}} \left(e^{\left[-\frac{1}{2\sigma^2}(x-x_0)^2 + i\frac{2\pi}{h}mv(x-x_0) \right]} + e^{\left[-\frac{1}{2\sigma^2}(x+x_0)^2 + i\frac{2\pi}{h}mv(x+x_0) \right]} \right) \tag{33}$$

and by an inverse Fourier transform:

$$\phi(p) = \frac{\sigma\sqrt{2\pi}}{\sqrt{2}h} e^{\left(-\frac{1}{2}\frac{1}{\left(\frac{h}{2\pi\sigma}\right)^2}(p-mv)^2 \right)} \left(e^{\left(-i\frac{2\pi}{h}px_0\right)} + e^{\left(+i\frac{2\pi}{h}px_0\right)} \right) \tag{34}$$

The wave function in the p representation is:

$$\varphi(p,t) = \frac{\sigma 2\sqrt{\pi}}{\sqrt{h}} e^{\left[-\frac{1}{\left(\frac{h}{2\pi\sigma}\right)^2}(p-mv)^2 - i\frac{2\pi}{h}\frac{p^2}{2m}t) \right]} \cos\left(\frac{2\pi}{h}px_0 \right) \tag{35}$$

and, taking into account the Jacobian, the spectral model's velocity distribution is:

$$\rho_s(v_s,t) = m\sigma \left(\frac{4\pi\sigma}{h} \right) e^{\left[-\frac{1}{2\left(\frac{h}{4\pi\sigma}\right)^2}(v_s-v)^2 \right]} \cos^2\left(\frac{2\pi}{h}mv_s x_0 \right) \tag{36}$$

To determine $\rho_f(v_f,t)$, we apply the method from **Section 3** using Equations (22, 23). As previously, $\sqrt{\left(\sigma^2 - i\frac{ht}{2\pi m}\right)} = r(t)e^{-i\theta(t)}$, where $\tan(2\theta(t)) = \frac{ht}{2\pi m\sigma^2}$, and :

$$R_{\pm}(x,t) = \frac{\sqrt{\sigma}}{\sqrt[4]{\left(\sigma^2 + \left(\frac{ht}{2\pi m\sigma}\right)^2\right)}} \exp\left[-\frac{1}{2}\frac{(x \pm x_0 - vt)^2}{\sigma^2 + \left(\frac{ht}{2\pi m\sigma}\right)^2} \right] \tag{37}$$

$$S_{\pm}(x,t) = \frac{h}{2\pi}\theta(t) + mv\left(x \pm x_0 - \frac{v}{2}t\right) + \frac{m\,t}{2}\frac{(x \pm x_0 - vt)^2}{\sigma^2 + \left(\frac{h}{2\pi m\sigma}\right)^2 t^2}\left(\frac{h}{2\pi m\sigma}\right)^2 \tag{38}$$

$$\psi(x,t) = \frac{1}{\sqrt{2}}\left(R_+(x,t)e^{i\frac{2\pi}{h}S_+(x,t)} + R_-(x,t)e^{i\frac{2\pi}{h}S_-(x,t)}\right) \tag{39}$$

We combine the terms of this expression to retrieve the "phase-amplitude" parameterization (3). For simplicity, we assume that the amplitude terms factorize as $R_+(x,t) \simeq R_-(x,t)$ if $x_0 = 0$:

$$\psi(x,t) = R(x,t)e^{i\frac{2\pi}{h}S(x,t)}$$

$$\psi(x,t) = \frac{\sqrt{\frac{\sigma}{2}}}{\sqrt[4]{\left(\sigma^2 + \left(\frac{ht}{2\pi m\sigma}\right)^2\right)}} e^{-\frac{1}{2}\frac{(x-vt)^2}{\sigma^2 + \left(\frac{ht}{2\pi m\sigma}\right)^2}} \left(e^{i\frac{2\pi}{h}S_+(x,t)} + e^{i\frac{2\pi}{h}S_-(x,t)}\right) \tag{40}$$

We factorize and find:

$$\frac{S_+(x,t) + S_+(x,t)}{2} =$$

$$\frac{h}{2\pi}\theta(t) + mv\left(x - \frac{v}{2}t\right) + \frac{m\,t}{2}\frac{(x-vt)^2 + (x_0)^2}{\sigma^2 + \left(\frac{h}{2\pi m\sigma}\right)^2 t^2}\left(\frac{h}{2\pi m\sigma}\right)^2$$

and

$$\frac{S_+(x,t) - S_+(x,t)}{2} = mvx_0 + m\,t\frac{x_0(x-vt)}{\sigma^2 + \left(\frac{h}{2\pi m\sigma}\right)^2 t^2}\left(\frac{h}{2\pi m\sigma}\right)^2$$

From this, by Equation (8), we deduce that:

$$v_f(x,t) - v = +\,t\frac{x - vt}{\sigma^2 + \left(\frac{h}{2\pi m\sigma}\right)^2 t^2}\left(\frac{h}{2\pi m\sigma}\right)^2 \tag{41}$$

thus

$$\frac{(x-vt)^2}{\sigma^2+\left(\frac{h}{2\pi m\sigma}\right)^2 t^2} = \frac{1}{t^2\left(\frac{h}{2\pi m\sigma}\right)^4}(v_f-v)^2\left(\sigma^2+\left(\frac{h}{2\pi m\sigma}\right)^2 t^2\right)$$

In this simplified model, the Jacobian has the same expression as that obtained for 1 slit:

$$J(t) = \frac{\partial v_f(x,t)}{\partial x} = \frac{t}{\sigma^2+\left(\frac{h}{2\pi m\sigma}\right)^2 t^2}\left(\frac{h}{2\pi m\sigma}\right)^2$$

and the correspondence between x and v_f leads to:

$$(x-vt) = \frac{\left(\sigma^2+\left(\frac{ht}{2\pi m\sigma}\right)^2\right)t}{\left(\frac{ht}{2\pi m\sigma}\right)^2}(v_f-v)$$

Finally, the velocity distribution for the fluid model is:

$$\rho_f(v_f,t) = \frac{1}{2}\frac{t\sigma\sqrt{\sigma^2+\left(\frac{h}{2\pi m\sigma}\right)^2 t^2}}{\left(\frac{h}{2\pi m\sigma}\right)t^2}\, e^{-\frac{\sigma^2+\left(\frac{h}{2\pi m\sigma}\right)^2 t^2}{t^2\left(\frac{h}{2\pi m\sigma}\right)^4}(v_f-v)^2}\cos\left(\frac{2\pi}{h}mv_f x_0\right)$$

This expression, aside from the modulation term, has the same limits in terms of t as the expression obtained in (27) for 1 slit. Therefore, one can also discriminate between the two models by the shape of their velocity distributions, as illustrated bellow.

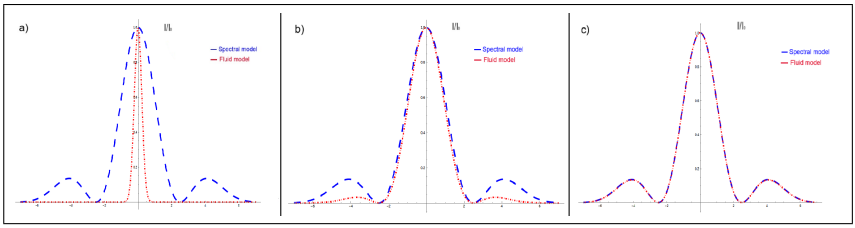

Figure 4: Plot of the velocity distribution of the two models after passing through two slits for near-field (a), intermediate (b), and far-field (c) regimes.

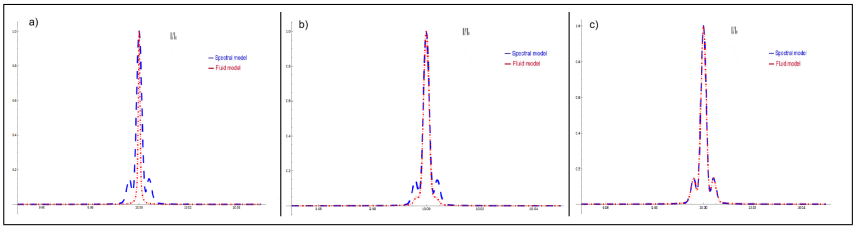

Figure 5: Plot of the Voigt profile (for $\gamma = \sigma/100$) of the two models after passing through two slits for near-field (a), intermediate (b), and far-field (c) regimes.

7 Conclusion

We have shown, in the case of a coherent atomic beam with a Gaussian transverse profile, that the spectral model and the fluid model of quantum mechanics do not lead to identical velocity distributions.

Although both profiles are the same in the far field, they differ notably in the near field, close to the beam's nozzle. It is possible to test these two models through a laser spectroscopy experiment, provided that the Voigt formula remains valid regardless of the model. It would also be possible to test the velocity distribution by placing a Stern-Gerlach magnet at different positions along the beam and analysing the resulting deflection directly [5] or through atomic interferometry [23].

The solutions we present offer a means for experimental testing of the two models of quantum mechanics, while remaining within the quantum mechanics framework. Such tests could provide experimental differenti-

ation between the two models. And to the best of our knowledge, this point has not been addressed in this context, where the focus is typically on trajectories.

Of course, it is not clear that the velocity distribution of the fluid model can be used in the Voigt formula without revisiting the theory of matter-radiation interaction, including the center-of-mass motion of the atoms. And if one seeks to reconcile the fluid model with the spectral model, whose results seem to be firmly established, it may be necessary to employ the fluid model with other solutions than the regular solutions of the Schrödinger equation [13, 24] .

Acknowledgments: Jacques Robert would like to thanks Chieko Kojima for providing access to the Japanese articles of T. Takabayasi.

References

[1] Louis de Broglie "Quanta de lumière, diffraction et interférences" Comptes rendus T.177 548(1923)
[2] M.V. Berry Phil.Trans. R. Soc. Lond. A 360, 1023 (2002)
[3] Newton, I. 1730 Opticks: or a treatise of the reflections, inflections and colours of light.
[4] C. Philippidis et al. Nuovo Cimento 52, 15 (1979)
[5] B.G. Englert et al. , Z. Naturforsch. 47, 1175 (1992)
[6] Scully, M., Phys. Scr. , 76, 41 (1998)
[7] Basil J. Hiley and Peter Van Reeth, Entropy , 20, 353 (2018)
[8] L. de Broglie, Ann. de Physique 3, 22 (1925).
[9] E. Schrödinger, Ann. d. Physik 79, 361, 489, 734; 80, 437 81, 109 (1926); Die Naturwissenschaften 14, 664 (1926).
[10] W. Heisenberg : The Physical Principles of the Quantum Theory, Dover Publications, Inc., New York (1949).
[11] C. G. Darwin, Roy. Soc. Proc. A117, 258 (1927)
[12] E. H. Kennard, Zeits. f. Physik 44, 326 (1927); Phys.Rev. 31, 876 (1928)
[13] L. de Broglie, J. Phys. Radium 8, 225 (1927)
[14] E. Madelung, Z. Phys. 40, 322 (1926)
[15] L. Landau, J.Phys. JJ.S.S.R. 5, 71 (1941)
[16] T. Nishiyama, Prog. Theor. Phys. 7 , 417 (1952)
[17] T. Takabayasi , Prog. Theor. Phys. 8, 143 (1952)

[18] G. Nienhuis,J. Quant.Spectrosc. Radiat. Transfer 20, 275(1978)
[19] Ch. J. Bordé, C. R. Physique 10, 866 (2009)
[20] D. Bohm , Prog. Theor. Phys. 9, 273 (1953)
[21] T. Takabayasi , Prog. Theor. Phys. 9, 187 (1953)
[22] D. Bohm, Phys. Rev., 85(2), 166 (1952)
[23] J.Robert et al. , J. Phys. II, 4, 2061 (1994)
[24] A. M. Shaarawi et al., Phys. Lett. A, 188(3), 218 (1994)
[25] L. B. Felsen, J. Opt. Soc. Am., 66, 751 (1976)
[26] Eamond Lalor, J. Opt. Soc. Am., 58, 1235 (1968)
[27] P. Feron et al. Z. Phys. D - Atoms, Molecules and Clusters 10, 221(1988)
[28] C. Y. Chen et al., Review of Scientific Instruments 72, 271 (2001)
[29] Ch. Salomon and J. Dalibard, C. R. Acad. Sci. Paris, t. 306, Série II, 1319 (1988)
[30] S. Kocsis et al., Science, 332, 1170 (2011)

(Manuscrit reçu le 24 Septembre 2024)